PHYSICAL REVIEW D **96,** 096016 (2017)

Spontaneous spin polarization due to tensor self-energies in quark matter

Tomoyuki Maruyama[1,2] and Toshitaka Tatsumi[3,2]

[1]*College of Bioresource Sciences, Nihon University, Fujisawa 252-8510, Japan*
[2]*Advanced Science Research Center, Japan Atomic Energy Agency, Tokai, Naka, Ibaraki 319-1195, Japan*
[3]*Department of Physics, Kyoto University, Kyoto 606-8502, Japan*

(Received 18 April 2017; published 21 November 2017)

We study the magnetic properties of quark matter in the Nambu–Jona-Lasinio model with the tensor interaction. The spin-polarized phase given by the tensor interaction survives even when the quark mass is zero, while that given by the axial-vector interaction disappears. There are two kinds of spin-polarized phases: one appears in the chiral-broken phase, and the other in the chiral-restored phase where the quark mass is zero. The latter phase can appear independently of the strength of the tensor interaction.

DOI: 10.1103/PhysRevD.96.096016

I. INTRODUCTION

The discovery of magnetars [1,2], which are neutron stars with a super strong magnetic field, seems to revive an important question about the origin of the strong magnetic field in compact stars. Magnetars have a huge magnetic field of 10^{15} G and are grouped into a new class of compact stars. Many people usually assume that the conservation of magnetic flux during stellar evolution explains the magnetic field of pulsars. However, if we naively apply this hypothesis to magnetars, we immediately have a contradiction that their radius should be much less than the Schwarzschild radius. Thus, it may not be very easy to explain the strong magnetic field without considering properties of hadronic matter inside stars. We should pay attention to a microscopic origin to solve the "magnetar" problem.

Recently, many theoretical and experimental efforts have been devoted to exploring the QCD phase diagram in the density-temperature (ρ-T) plane, which may be closely related to phenomena observed in relativistic heavy-ion collisions, compact stars, or the early Universe [3–5]. In particular, quark-gluon plasma (QGP) at a high-temperature but low-density regime and color superconductivity (CSC) at a high-density but low-temperature regime have been elaborately studied [3,6].

Because dense matter occupies a large portion of compact stars, its property should be reflected in various phenomena. Tatsumi [7] has suggested the possibility of a ferromagnetic transition in QCD; it is possible in quark matter interacting with a one-gluon-exchange (OGE) interaction and its critical density is of the order of nuclear density, $\rho_{FM} \simeq \rho_0$, where ρ_0 is the normal nuclear matter density, $\rho_0 \sim 0.16$ fm^{-3}. Using this idea we can roughly estimate the strength of the magnetic field at the surface of compact stars. Considering a star with mass, $M \sim 1.4\ M_\odot$, and radius, $R \sim 10$ Km, and assuming the dipole magnetic field, the maximum strength at the surface can be simply estimated by $B_{\max} = (8\pi/3) f_Q \mu_q \rho_0$, where f_Q is the volume fraction of quark matter, and μ_q is the quark magnetic moment. Thus we evaluate it as $O(10^{15\text{–}17}\ \mathrm{G})$ for the extreme case, $f_Q = 1$, which should be compared with observations. This is a perturbative result based on the Bloch mechanism, in analogy with electron gas [8–10].

In the relativistic framework the "spin density" can take two forms [11], $\psi^\dagger \Sigma^i \psi (\equiv -\bar{\psi}\gamma_5\gamma^i\psi)$ and $\psi^\dagger\gamma^0\Sigma^i\psi(\equiv -\bar{\psi}\sigma^{12}\psi)$, with ψ being the quark field. The former is a space component of the axial-vector (AV) mean field, and the latter is that of the tensor (T) one. These two mean fields become equivalent to each other in the non-relativistic limit, while they are quite different in the ultrarelativistic limit (massless limit) [11]. In the text we shall call the former and latter polarizations the AV-type and T-type spin polarizations (SP), respectively.

For quark matter, we have introduced the AV interaction and have studied the SP mechanism in the mean-field approximation [7,12,13]. In these studies we have succeeded at showing the coexistence of the spin polarization and the CSC [14] and the dual chiral density wave (DCDW), which is an inhomogeneous chiral phase [13,15].

Furthermore, Maedan has also studied the SP in the Nambu–Jona-Lasinio (NJL) model [16] with this AV mean field [17]. When the quark mass is fixed, the SP appears in a high-density region, but the AV mean field disappears when the quark mass becomes zero. Then, the spin-polarized phase can appear only in a low-density region just below the chiral phase transition (CPT) density, ρ_c.

As mentioned above, the AV channel of the quark interactions has often been used for the study of SP in quark matter because this channel is obtained by the Fierz transformation from the OGE interaction. On the other hand, the T channel has not been often used because this interaction channel does not appear in the Fierz transformation from the OGE interaction.

The OGE interaction should be useful in a very high-temperature and/or very high-density region. However, the density region is not very high around the CPT

density, and a perturbative calculation cannot be applied there. In such a moderate density region, the low-energy effective models such as the NJL model have often been used, but they are not directly related to the OGE interaction. They include some nonperturbative effects instead, and there is no reason to exclude this channel.

The T channel interaction can play an important role, differently from the AV channel interaction, to produce the spin-polarized phase, because the T-type SP can appear even if the quark mass becomes zero [12]. Actually, Tsue *et al.* [18] have also shown that the SP appears in the chiral-restored phase, where the quark mass is zero, in the NJL model within the effective potential approach.

In addition, the magnetic effect with the T-type SP is much larger than that of the AV-type SP [12]. In the Fermi degenerate system, the magnetic field should be almost created by magnetization, which is proportional to $\psi^\dagger\gamma^0\Sigma^i\psi$. The lower component of the Dirac spinor contributes to $\psi^\dagger\Sigma^i\psi$ and $\psi^\dagger\gamma^0\Sigma^i\psi$, oppositely. In the relativistic region, where the quark mass is much less than the Fermi momentum, the contribution from the lower component has the same order as that from the upper component. As $\langle\psi^\dagger\Sigma^i\psi\rangle$ increases, then $\langle\psi^\dagger\gamma^0\Sigma^i\psi\rangle$ becomes smaller in the AV-type SP.

Thus, the AV-type SP appears in a narrow density region below the chiral transition and may not contribute to the magnetic field very largely. In contrast, the T-type SP can appear in the wide density region and largely contribute to the magnetic field. Thus, we should examine behaviors of the SP and its relation with chiral symmetry.

We discuss spontaneous spin polarization in the absence of the external magnetic field. If quark matter is exposed to the strong external magnetic field, we must take into account the coupling with it; the energy scale of $O(10^{18-19})$G is comparable with the Fermi energy or the dynamical quark mass.

In this paper we study the T-type SP in the NJL model and figure out the relation between the spontaneous SP and chiral transition. In the next section we present a framework to deal with the present subject. In Sec. III we show the results of the numerical calculation and discuss the relation between SP and chiral restoration. Section IV is devoted to summary and concluding remarks.

II. FORMALISM

In order to examine the T-type SP we start with the following NJL-type Lagrangian density with $SU(2)$ chiral symmetry,

$$\mathcal{L} = \mathcal{L}_K + \mathcal{L}_s + \mathcal{L}_V + \mathcal{L}_T, \tag{1}$$

with

$$\mathcal{L}_K = \bar\psi(i\partial\!\!\!/ - m)\psi, \tag{2}$$

$$\mathcal{L}_S = -\frac{G_s}{2}[(\bar\psi\psi)^2 + (i\bar\psi\gamma_5\tau\psi)^2], \tag{3}$$

$$\mathcal{L}_V = -\frac{G_v}{2}[(\bar\psi\gamma_\mu\psi)(\bar\psi\gamma^\mu\psi) + (i\bar\psi\gamma_5\gamma_\mu\tau\psi)(i\bar\psi\gamma^\mu\gamma_5\tau\psi)], \tag{4}$$

$$\mathcal{L}_T = -\frac{G_T}{2}[(\bar\psi\sigma_{\mu\nu}\psi)(\bar\psi\sigma^{\mu\nu}\psi) + (\bar\psi i\tau_a\gamma_5\sigma_{\mu\nu}\psi)(\bar\psi i\tau_a\sigma^{\mu\nu}\gamma_5\psi)], \tag{5}$$

where ψ is a field operator of quarks, and G_s, G_v, and G_T are the coupling constants for the scalar, vector, and tensor channels, respectively.

Here, we comment on the tensor interaction. If the original Lagrangian includes only $\mathcal{L}_S$ in Eq. (3), the Fierz transformation effectively gives the following Lagrangian:

$$\begin{aligned}\mathcal{L}_{FT} = \frac{1}{4}G_s[&(\bar\psi\psi)^2 + (\bar\psi i\tau\gamma_5\psi)^2 - (\bar\psi\tau\psi)^2 - (\bar\psi i\gamma_5\psi)^2 \\ &+ 2(\bar\psi\gamma_5\gamma_\mu\psi)(\bar\psi\gamma_5\gamma^\mu\psi) - 2(\bar\psi\gamma_\mu\psi)(\bar\psi\gamma^\mu\psi) \\ &+ \frac{1}{2}(\bar\psi\sigma_{\mu\nu}\psi)(\bar\psi\sigma^{\mu\nu}\psi) - \frac{1}{2}(\bar\psi\sigma_{\mu\nu}\tau\psi)(\bar\psi\sigma^{\mu\nu}\tau\psi)].\end{aligned} \tag{6}$$

Thus, the tensor interaction can appear even if the original interaction does not include this channel. However, one cannot derive any channel of the interactions in the NJL model from basic QCD. We calculate here the spin polarization by using several values of G_T to see G_T dependence.

In the present work, we restrict calculations and discussions to the flavor symmetric matter ($\rho_u = \rho_d$) at zero temperature. Within the mean-field approximation, the quark Dirac spinor $u(\boldsymbol{p}, s)$ is obtained as the solution of the following equation,

$$[p\!\!\!/ - M_q - U_0\gamma^0 - U_T\Sigma_z]u(\boldsymbol{p}, s) = 0, \tag{7}$$

with $\Sigma_z = \mathrm{diag}(1, -1, 1, -1)$ and

$$M_q = -G_s\rho_s = -G_s\langle\bar\psi\psi\rangle, \tag{8}$$

$$U_0 = G_v\rho_q = G_v\langle\bar\psi\gamma^0\psi\rangle, \tag{9}$$

$$U_T = G_T\rho_T = G_T\langle\bar\psi\Sigma_z\psi\rangle - G_T\langle\bar\psi\Sigma_z\tau_3\psi\rangle\tau_3. \tag{10}$$

Accordingly the quark Green function is defined as a solution of the following equation:

$$[p\!\!\!/ - M_q - U_0\gamma^0 - U_T\Sigma_z]S(p) = 1. \tag{11}$$

By solving the above Eq. (11) we can obtain

$$S(p)=\frac{[\gamma_\mu p^{*\mu}+M_q+\Sigma_z U_T]\{p^{*2}-M_q^2+U_T^2+2U_T(p_z\gamma_5\gamma^0-p_0\gamma_5\gamma^3)\}}{(p_0^{*2}-E_p^2-U_T^2)^2-4U_T^2(\boldsymbol{p}_T^2+M_q^2)\pm i\delta}, \tag{12}$$

with $p_\mu^*=p_\mu-U_0\delta_\mu^0$ and $E_p=\sqrt{\boldsymbol{p}^2+M_q^2}$.

The $S(p)$ has poles at $p_0=\pm e(\boldsymbol{p},s)$, which give the single particle energies

$$\begin{aligned}e(\boldsymbol{p},s)&=\sqrt{\left(\sqrt{M_q^2+\boldsymbol{p}_T^2}+sU_T\right)^2+p_z^2}+U_0\\&=\sqrt{E_p^2+2sU_T\sqrt{M_q^2+\boldsymbol{p}_T^2}+U_T^2}+U_0,\end{aligned} \tag{13}$$

where $s=\pm1$ indicates the spin of a quark.

It should be interesting to compare it with a single particle energy in the AV mean field, U_A:

$$\begin{aligned}e(\boldsymbol{p},s)&=\sqrt{\left(\sqrt{M_q^2+p_z^2}+sU_A\right)^2+\boldsymbol{p}_T^2}+U_0\\&=\sqrt{E_p^2+2sU_A\sqrt{M_q^2+p_z^2}+U_A^2}+U_0.\end{aligned} \tag{14}$$

Here, we make a comment on the qualitative difference in the SP by the tensor and axial-vector interactions. When $U_A=U_T$, we can obtain the above expression of $e(\boldsymbol{p},s)$ in Eq. (14) from that in Eq. (13) by exchanging p_z and p_T. The equal-energy surfaces in the momentum space satisfy the same relation for the two types of SP. However, p_z is one-dimensional, while p_T is the absolute value of the two-dimensional vector.

In Fig. 1, we show the equal-energy surface for $e(\boldsymbol{p},-1)-U_0=3M_q$ (a) in the T-type spin-polarized phase when $U_T=3M_q$ and (b) in the AV-type spin-polarized phase when $U_A=3M_q$. We see that difference in the momentum distribution between the two types of SP: it is deformed prolately in the T-type SP and oblately in the AV-type SP.

Using these single particle energies, the quark propagator is separated into the vacuum part S_F and the density-dependent part S_D as

$$S(p)=S_F(p)+S_D(p), \tag{15}$$

with

$$S_F(p)=\frac{[\gamma^\mu p_\mu^*+M_q+\Sigma_z U_T]\{p^2-M_q^2+U_T^2+2U_T(p_z\gamma_5\gamma^0-p_0\gamma_5\gamma^3)\}}{[p_0^2-e^{*2}(\boldsymbol{p},1)+i\delta][p_0^2-e^{*2}(\boldsymbol{p},-1)+i\delta]}, \tag{16}$$

$$S_D(p)=\sum_{s=\pm1}[\gamma_0 e^*-\boldsymbol{\gamma}\cdot\boldsymbol{p}+M_q+\Sigma_z U_T]\left\{1+\frac{s(p_z\gamma_5\gamma^0-p_0\gamma_5\gamma^3)+sU_T}{\sqrt{\boldsymbol{p}_T^2+M_q^2}}\right\}\frac{i\pi}{2e^*(\boldsymbol{p},s)}n(\boldsymbol{p},s)\delta[p_0-e(\boldsymbol{p},s)], \tag{17}$$

where $p_\mu^*-p_\mu-U_0\delta_\mu^0$; $e^*=e-U_0$; $n(\boldsymbol{p},s)=\Theta[e_F-e(\boldsymbol{p},s)]$; and e_F is the Fermi energy.

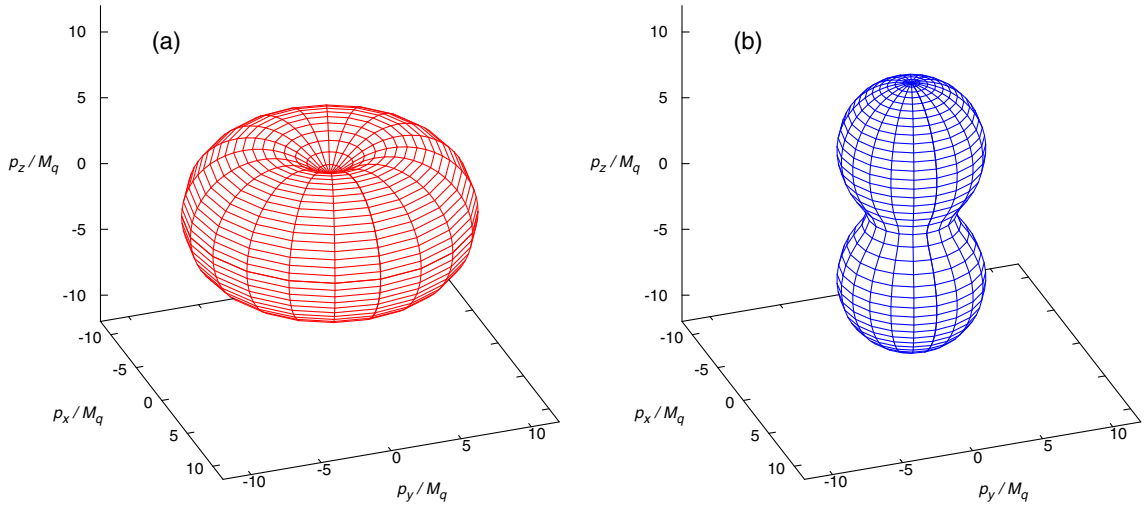

FIG. 1. The energy constant surfaces for $e-U_0=3M_q$ and $s=-1$, when (a) $U_T=3M_q$ and when (b) $U_A=3M_q$.

In the above expression, the quark density is written as

$$\rho_q = N_d \sum_{s=\pm 1} \int \frac{d^3p}{(2\pi)^3} \theta[e_F - e(\boldsymbol{p}, s)], \tag{18}$$

where $N_d = N_f N_c = 6$ is given by the degeneracy of the flavors, $N_f = 2$, and color degrees of freedom, $N_c = 3$; the baryon density is given as $\rho_B = \rho_q / N_c$.

Here, we make a comment about the vector interaction. The vector mean field, U_0, has only a role to shift the single particle energy, and the solutions of the mean-field equations (8) and (10) are not changed, so that the vector interaction does not affect a spin property. When $U_0 = 0$, the quark chemical potential, e_F, does not monotonously increase with density, and e_F becomes maximum at a certain density, which we call ρ_M. If this ρ_M is smaller than the CPT density, ρ_c, there are two solutions for a chemical potential. In the density region, $\rho_M < \rho_B < \rho_c$, $\partial e_F / \partial \rho_B < 0$, so that this state is unstable. As the chemical potential increases, thus, the system is transitioned to the chiral-restored phase at ρ_M; this phase transition is of the first order.

As the vector coupling G_v increases, the density dependence of e_F is changed, and the ρ_M becomes higher. When $\rho_M \geq \rho_c$, the system is continuously changed from the chiral-broken phase to the chiral-restored phase at $\rho_B = \rho_c$, so that the CPT is of the second order [19,20].

The nature of the CPT has not been clarified, yet. As mentioned above, we can control the CPT by varying G_v without changing other properties. In this work, thus, we assume that G_v is sufficiently large and that the CPT is of the second order. We omit U_0 and rewrite p_0^* and e^* as p_0 and e in the following. Then, we solve Eqs. (8) and (10) for the chiral-broken phase in all density regions. If one would like to describe the CPT as the first order phase transition, one should set the value of G_V to give any ρ_M and exclude the solutions in $\rho_M < \rho_B < \rho_c$.

In the mean-field approximation the dynamical quark mass M_q and the U_T are determined by

$$1 - \frac{G_s \rho_s}{M_q} = 0, \tag{19}$$

$$1 - \frac{G_T \rho_T}{U_T} = 0, \tag{20}$$

where the scalar density ρ_s and the tensor density ρ_T are given by

$$\rho_s = N_d \int \frac{d^4p}{(2\pi)^4} \mathrm{Tr}[iS(p)], \tag{21}$$

$$\rho_T = N_d \int \frac{d^4p}{(2\pi)^4} \mathrm{Tr}[i\Sigma_z S(p)]. \tag{22}$$

Each density is separated into two parts, the vacuum part and the density-dependent part such as

$$\begin{aligned}\rho_s &= \rho_s(V) + \rho_s(D) \\ &= N_d \int \frac{d^4p}{(2\pi)^4} \mathrm{Tr}[iS_F(p)] + N_d \int \frac{d^4p}{(2\pi)^4} \mathrm{Tr}[iS_D(p)].\end{aligned} \tag{23}$$

The density-dependent part is written as

$$\rho_s(D) = N_d \sum_{s=\pm 1} \int \frac{d^3p}{(2\pi)^3} n(\boldsymbol{p}, s) \frac{M_q}{e(\boldsymbol{p}, s)} \left(1 + \frac{s U_T}{\sqrt{M_q^2 + p_T^2}} \right). \tag{24}$$

The density-dependent part of the tensor density is also written as

$$\rho_T(D) = N_d \sum_{s=\pm 1} \int \frac{d^3p}{(2\pi)^3} n(\boldsymbol{p}, s) \frac{s\sqrt{\boldsymbol{p}_T^2 + M_q^2} + U_T}{e(\boldsymbol{p}, s)}. \tag{25}$$

Because $\rho_T < 0$ when $U_T > 0$, thus Eq. (20) has a solution when $G_T < 0$.

Here, we make a comment on the tensor density. When $M_q = 0$, the tensor density in Eq. (25) becomes

$$\rho_T(D) = -\frac{N_d}{12\pi} e_F^3 \neq 0, \tag{26}$$

while $\rho_A = 0$ [13,14]. When $M_q = 0$, namely, the T-type SP can appear while the AV-type SP never appears. This difference comes from the momentum distribution in the SP phase (see Fig. 1).

The above argument about the sign of G_T is right only when the SP is isoscalar, where the average spins of u- and d-quarks are directed along the same direction. In the isovector spin-polarized system, the tensor densities for the u- and d-quarks have opposite signs. In the symmetric matter, we define $\rho_T = \rho_T(u) - \rho_T(d) = 2\rho_T(u)$ and $U_T = U_T(u) - U_T(d) = 2U_T(u)$, and we rewrite Eq. (10) as $U_T = -G_T \rho_T$, which is the same as Eq. (20) except for the sign of the rhs. This fact demonstrates that, when $G_T > 0$, the isovector spin-polarized phase can appear, and its strength is the same as that for $G_T < 0$.

In this paper we perform the argument only when $G_T < 0$, but we can apply the same argument to the isovector spin-polarized system for $G_T > 0$ and get the same strength of the SP for each quark. However, we should note that a magnetization is larger when $G_T > 0$, because of the opposite sign for the u- and d-quark charges.

In order to extract the vacuum part we use the proper time regularization (PTR) [21], where the thermodynamical potential density is written with the cutoff parameter Λ as

$$\begin{aligned}\Omega_{\rm vac} &= iN_d \int \frac{d^4p}{(2\pi)^4} \ln\left[(p_0^2 - e^2(\boldsymbol{p},+1))\right]\left[(p_0^2 - e^2(\boldsymbol{p},-1))\right] \\ &= -iN_d \sum_{s=\pm 1} \int_0^\infty \frac{d\tau}{\tau} \int \frac{d^4p}{(2\pi)^4} e^{\tau[(p_0^2 - e^2(\mathbf{p},s))]} \\ &\approx \frac{N_d}{8\pi^2} \sum_s \int_{1/\Lambda^2}^\infty \frac{d\tau}{\tau^2} \int_{M_q}^\infty dE_T E_T e^{-\tau(E_T + sU_T)^2} \end{aligned} \tag{27}$$

at zero temperature. The vacuum part of the scalar density is then given by

$$\begin{aligned}\rho_s(V) &= \frac{\partial \Omega_{\rm vac}}{\partial M_q} \\ &= -\frac{N_d M_q}{8\pi^2} \sum_s \int_{1/\Lambda^2}^\infty \frac{d\tau}{\tau^2} e^{-\tau(M_q + sU_T)^2} \\ &= -\frac{N_d M_q}{8\pi^2} \Lambda^2 \sum_s F_2\left(\frac{(M_q + sU_T)^2}{\Lambda^2}\right), \end{aligned} \tag{28}$$

where the function F_n is defined as

$$F_n(x) = x \int_x^\infty \frac{d\tau}{\tau^n} e^{-\tau}. \tag{29}$$

The vacuum part of the tensor density can be also obtained with $\rho_T(V) = \partial \Omega_{\rm vac}/\partial U_T$. However, this term strongly depends on the cutoff parameter Λ in the present model, even when $M_q = 0$. Indeed, the vacuum part of the tensor density is also dependent on the regularization scheme and the value of the cutoff parameter (see Appendix B 1 for details). For example, the vacuum contribution in the PTR suppresses the SP while that in the effective potential approach [18] enlarges it.

In the AV-type SP, the vacuum part in the PTR also suppresses the SP [13], while that in the momentum cutoff enlarges it [17].

The cutoff parameter has a role to restrict the momentum space in the calculation. The T and AV densities are given by the difference between the spin-up and spin-down contributions, which depends on the restriction of the momentum space, so that the result sensitively depends on the regularization method and the value of the cutoff parameter.

In the usual renormalization procedure we regularize the vacuum polarization by introducing the suitable counterterms which are determined from physical values. In order to regularize the tensor density, $\rho_T(V)$, we need to introduce at least three counterterms which are proportional to U_T^2, U_T^4, and $U_T^2 M^2$. In the NJL model we regularize the vacuum contributions by using a cutoff parameter. The vacuum part of the scalar density is associated with the dynamical quark mass in the vacuum but is not concerned with the spin properties. In the present model, the vacuum part of the tensor density strongly diverges as $\Lambda \to \infty$ for a small asymmetry of the spin states. This fact does not have any physical meaning, but we do not have any clear rule to regularize the tensor density in a systematic way.

Thus, the cutoff dependence of the tensor density from the vacuum contribution is less meaningful at present. In the NJL model it is not easy to apply a consistent method even for the qualitative discussions. In the next section, then, we perform an actual calculation without the vacuum contribution for the tensor density: $\rho_T \approx \rho_T(D)$.

In Appendix B 2, instead, we try to give a tentative calculation for the SP including the vacuum contribution.

III. RESULTS

In this section we show some numerical results for the SP in relation to the chiral transition. For this purpose, we consider the chiral limit and use two kinds of the parameter sets PM1 ($G_s\Lambda^2 = 6, \Lambda = 850$ MeV) and PM2 ($G_s\Lambda^2 = 6.35, \Lambda = 660.37$ MeV), which are determined to reproduce the vacuum properties such as the pion decay constant, constituent quark mass, scalar condensate, and so on [13].

Before showing actual numerical results, we discuss the critical density of the SP (ρ_{SC}).

The tensor mean field is determined by the following self-consistent equation[1]:

$$F_T(U_T) = 1 - \frac{G_T \rho_T}{U_T} = 0. \tag{30}$$

When $U_T \gg e_F + M_q$, $\rho_T = -N_d e_F^3/12\pi$, and $\rho_q = N_d U_T e_F^2/4\pi$ (see Appendix A), then $e_F \to 0$ and $F_T(U_T) \to 1$ when $U_T \to \infty$ at the fixed density. Hence, Eq. (30) has a solution when $F_T(0) < 0$ at $U_T = 0$, which leads to

$$J = 1 + \frac{G_T N_d}{2\pi^2}\left\{ p_F E_F + \frac{M_q^2}{2} \ln\left(\frac{E_F + p_F}{E_F - p_F}\right)\right\} \le 0, \tag{31}$$

with p_F being the Fermi momentum and $E_F = e_F(U_T = 0) = \sqrt{p_F^2 + M_q^2}$.

$J = 0$ in Eq. (31) can be expressed by the two independent parameters, $M_q^2 G_T$ and p_F^c/M_q, where p_F^c indicates the critical Fermi momentum for the spontaneous SP. We show the boundary of the spin-polarized phase in Fig. 2.

In Fig. 3 we show $F_T(0)$ with (a) PM1 and (b) PM2 when $-G_T/G_s = 0.6 \sim -1.5$ as functions of baryon

[1] $\rho_T \to 0$ when $U_T \to 0$ in Eq. (25).

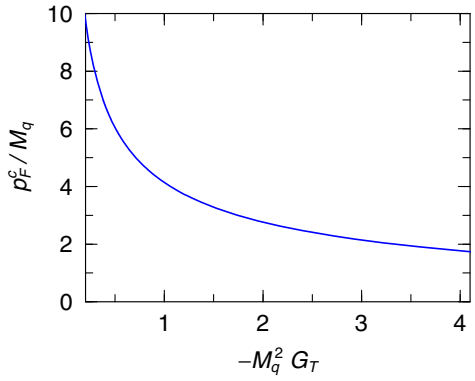

FIG. 2. Coupling constant versus the critical Fermi momentum for the spontaneous spin polarization.

density, ρ_B, normalized by the normal nuclear density $\rho_0 = 0.17\ \mathrm{fm}^{-3}$. In addition, we show the dynamical quark mass normalized by nucleon mass M_N at the spin-saturated system ($\rho_T = 0$) with PM1 (solid line) and PM2 (long dashed line).

As baryon density becomes higher, $F_T(0)$ decreases at first and increases later, so that $F_T(0)$ has a maximum at CPT, ρ_c, and monotonously decreases again. For comparison, we show $F_T(0)$ when $M_q = 0$ with thin lines, where we plot the results only when $G_T = -1.5G_s$ for PM1 and $G_T = -1.2G_s$ for PM2. We see that $F_T(0)$ monotonously decreases when $M_q = 0$ with the increase of ρ_B.

It was shown in Ref. [12] that $F_T(0)$ monotonously decreases with density when the dynamical quark mass M_q is fixed. However, the dynamical quark mass is also decreasing in the NJL model, and a smaller quark mass enlarges $F_T(0)$. This effect changes the density dependence of $F_T(0)$, which becomes minimum at a certain density and subsequently increases. Because $\partial M_q/\partial\rho_B$ is not continuous at $\rho_B = \rho_c$, the maximum point of $F_T(0)$ becomes a cusp, which indicates that the CPT is of the second order.[2]

As mentioned before, $F_T(0) = 0$ shows the critical density of the phase transition between the spin-saturated and spin-polarized phases. As the coupling $-G_T$ becomes larger, the number of crossing points becomes 1, 3, and 1. The last case, where the number of crossing points is 1, indicates that $F_T(0) < 0$ at $\rho_B = \rho_c$. In this case the line of $F_T(0)$ with $M_q = 0$ also crosses zero at a density lower than the CPT density (see the thin lines in Fig. 3).

These results suggest that there are two kinds of spin-polarized phases: one is the chiral-broken SP (SP-I) which appears in the chiral-broken phase, $M_q > 0$, and the other is the chiral-restored SP (SP-II) which appears in the chiral-restored phase, $M_q = 0$. Here we define $\rho_{SC}^{(\mathrm{I})}$ and $\rho_{SC}^{(\mathrm{II})}$ as critical densities of the SP-I and SP-II phases, respectively.

[2]If the phase transition is of the first order, the critical density of the chiral phase transition is lower than that of the second order.

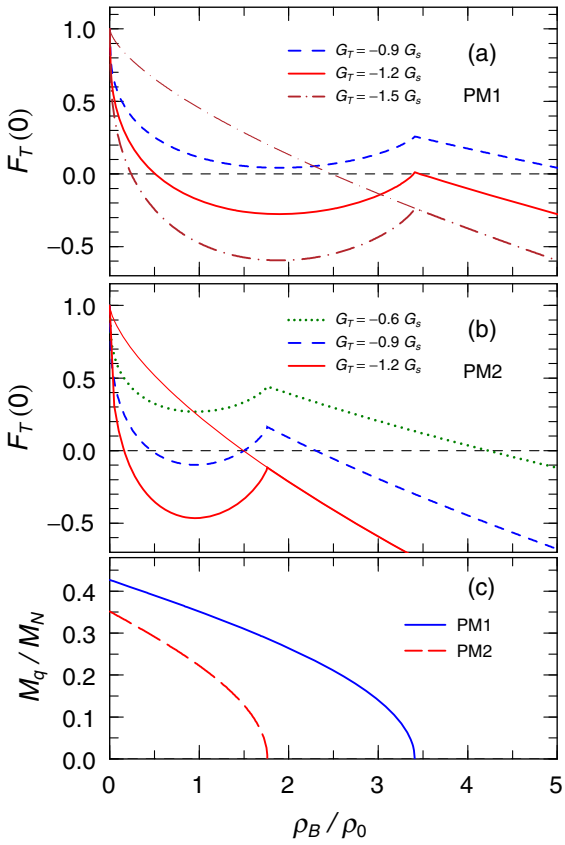

FIG. 3. $F_T(0)$ with (a) PM1, (b) PM2, and (c) the dynamical quark mass as functions of ρ_B/ρ_0. In panel (a) the dashed, solid and dotted-dashed lines represent the results results when $G_T/G_s = -0.9$, -1.2 and -1.5, respectively. In panel (b) the dotted line represents the result when $G_T/G_s = -0.6$, and the dashed and solid lines are the same as those in panel (a). The thin lines in panels (a) and (b) indicate $F_T(0)$ when $M_q = 0$. In panel (c), the solid and long dashed lines indicate M_q/M_N with PM1 and PM2, respectively.

$\rho_{SC}^{(\mathrm{II})}$ exists for any G_T, but $\rho_{SC}^{(\mathrm{I})}$ appears only when $-G_T$ is large; namely, the SP-II phase always appears independently of the strength of the tensor interaction. In addition, $-G_T$ becomes even larger, such that $F_T(0) < 0$ at $\rho_B = \rho_c$ $\rho_{SC}^{(\mathrm{II})} < \rho_c$; here, we should note that $M_q = 0$ is a solution of Eq. (8) as well as a solution of the gap equation (19).

In Fig. 4, we show [(a) and (c)] the baryon density dependence of the tensor density ρ_T/ρ_0 with PM1 and [(b) and (d)] that of the dynamical quark mass when [(a) and (b)] $G_T = -1.2G_s$ and [(c) and (d)] $G_T = -1.5G_s$. In panels (a) and (c), the solid lines represent $\rho_T/(N_c\rho_0)$ in the spin-polarized phase when $M_q > 0$, and the dotted lines indicate that when $M_q = 0$. In panels (b) and (d), the solid and dashed lines represent the dynamical quark mass in the spin-polarized and spin-saturated phases, respectively.

When $G_T = -1.2G_s$ [Figs. 4(a) and 4(b)], we can see that the two kinds of spin-polarized phases, SP-I and SP-II, appear. In addition, there is a density region where the three

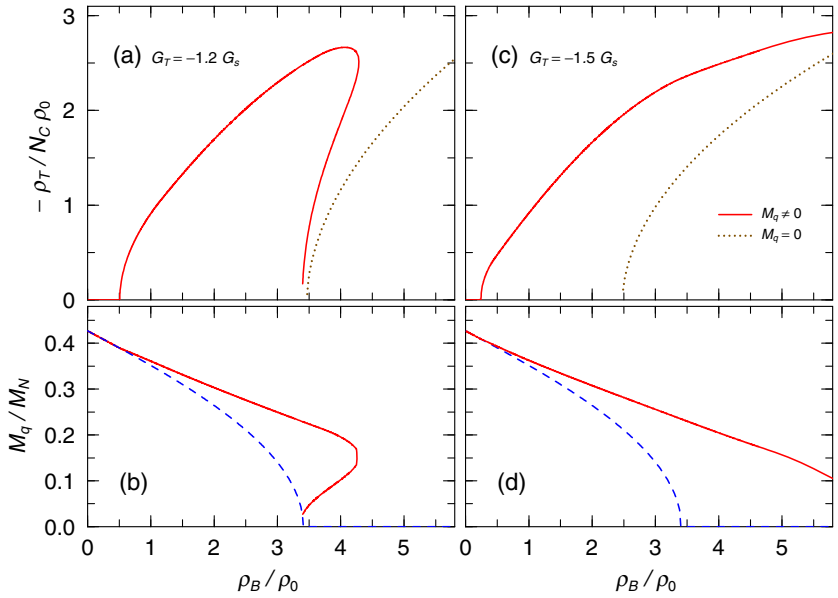

FIG. 4. Spin-polarization properties with PM1. (a) and (c): The tensor densities normalized by the normal nuclear density. The solid and dotted lines represent the results in the chiral-broken and chiral-restored phases, respectively. (b) and (d): The dynamical quark mass normalized by nucleon mass in the spin-polarized (solid lines) and spin-saturated phases (dashed lines). The left and right panels show the results when [(a) and (b)] $G_T = -1.2$ and [(c) and (d)] $G_T = -1.5$, respectively.

solutions corresponding to the spin-polarized phases, two SP-I phases and one SP-II phase, exist.

When $G_T = -1.5G_s$ [Figs. 4(c) and 4(d)], the SP-I phase appears at first, and the SP-II phase appears in the density region, $\rho_B < \rho_c$. Both SP phases exist in the same density region up to a density higher than the *CPT* density, ρ_c, and the SP-I phase disappears at a density higher than ρ_c, where $M_q = 0$ and $U_T \neq 0$.

In this approach we discard the vacuum contribution to the tensor density even though the scalar density includes the vacuum part, so that we cannot define the total energy or determine what is realized among the spin-saturated, SP-I, and SP-II phases.

In order to look into this behavior more clearly, we calculate $F_T(U_T)$ by varying baryon density. In Fig. 5 we show the results at several baryon densities.

When $\rho_B \lesssim 2\rho_0$, $F_T(U_T)$ is a monotonously increasing function. As the density decreases, $F_T(0)$ becomes smaller, and, when $F_T(0) < 0$, the equation $F_T(U_T) = 0$ has a solution.

When $\rho_B \gtrsim 2\rho_0$, $F_T(0)$ becomes larger with density, but $F_T(U_T)$ has a minimum at a certain U_T. The equation $F_T(U_T) = 0$ has two solutions when $F_T(0) > 0$ and the minimum value is negative. As density further increases, the minimum value of F_T becomes positive, and there is no solution.

In Fig. 6, we show the results with PM2 with [(a) and (b)] $G_T = -0.8G_s$, [(c) and (d)] $G_T = -1.2G_s$, and [(e) and (f)] $G_T = -1.5G_s$. The behaviors of the SP are similar to those in PM1 (Fig. 4). When $G_T = -0.8G_s$ [Figs. 6(a) and 6(b)], the SP-I and SP-II phases appear in different density regions. When $G_T = -1.2G_s$ [Figs. 6(c) and 6(d)] and $G_T = -1.5G_s$ [Figs. 6(e) and 6(f)], the results clearly show that the SP-I and SP-II phases coexist in the density region, $\rho_B > \rho_c$, and that the SP-I phase disappears at higher density.

We can confirm that the SP-I phase disappears at a density higher than ρ_c, where the tensor density is finite, $\rho_T \neq 0$. In Fig. 7 we finally show the critical density between the spin-saturated and spin-polarized phases as a function of $G_T M_N^2$ in (a) the chiral-broken phase, $\rho_{SC}^{(\mathrm{I})}$, and

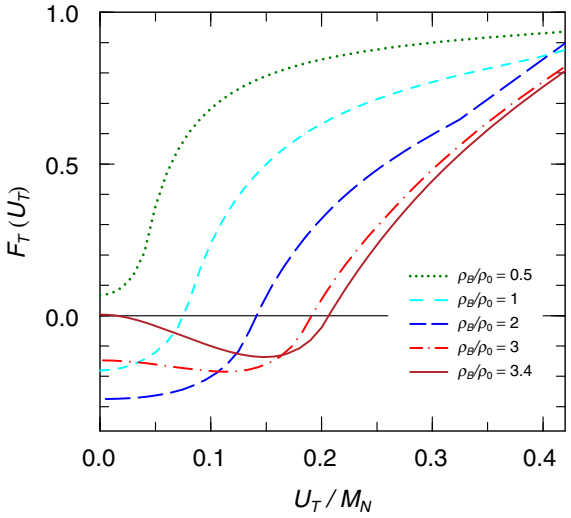

FIG. 5. $F_T(U_T)$ versus U_T/M_N with PM1 and $G_T = -1.2G_s$. The dotted, dashed, long-dashed, dotted-dashed, and solid lines represent results when $\rho_B/\rho_0 = 0.5$, 1, 2, 3, 3.4, respectively.

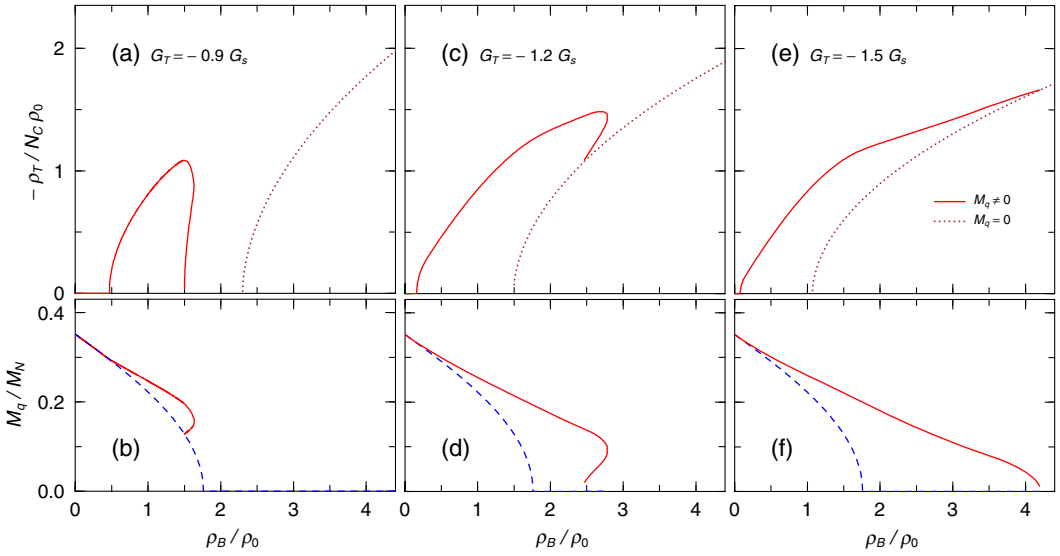

FIG. 6. Spin-polarization properties with PM2. (a), (c), and (e): The T densities normalized by the normal nuclear matter density. The solid and dotted lines represent the results in the chiral-broken and chiral-restored phases, respectively. (b), (d), (f): The dynamical quark mass normalized by nucleon mass in the spin-polarized (solid lines) and spin-saturated phase (dashed lines). The left, middle, and right panes show the results when [(a) and (b)] $G_T/G_s = -0.9$, [(c) and (d)] $G_T/G_s = -1.2$, and [(e) and (f)] $G_T/G_s = -1.5$, respectively.

(b) chiral-restored phase, $\rho_{SC}^{(\mathrm{II})}$. The critical density when $M_q = 0$, $\rho_{SC}^{(\mathrm{II})}$, is determined only by G_T, independently of G_s. In addition, we plot the critical density of CPT, ρ_c, with PM1 (dotted line) and PM2 (dashed line) in Fig. 7(b).

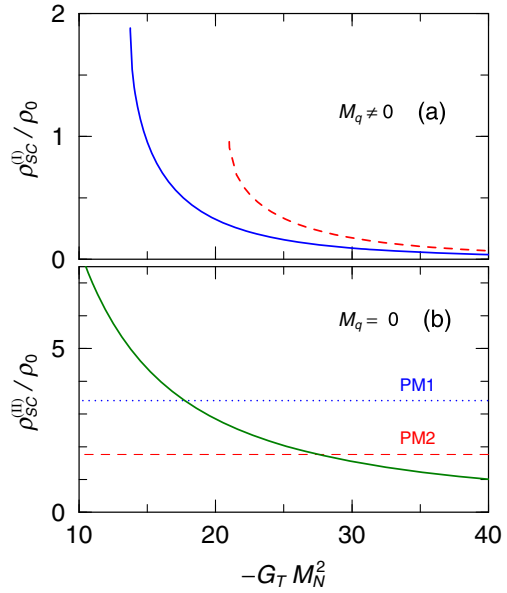

FIG. 7. Critical density between the spin-saturated and spin-polarized phases as functions of $G_T M_N^2$ when (a) $M_q \neq 0$ and (b) $M_q = 0$. In panel (a) the solid and dashed lines represent $\rho_{SC}^{(\mathrm{I})}/\rho_0$ with PM1 and PM2, respectively. In panel (b) the solid line shows the critical density of SP-II, $\rho_{SC}^{(\mathrm{II})}/\rho_0$, and the dotted and dashed lines indicate the critical densities of CPT, ρ_c/ρ_0, with PM1 and PM2, respectively.

We see the consequences in the phase diagram as follows. As $-G_T$ increases, the phase transition in the SP-I phase appears at $\rho_B \approx 1.9\rho_0$ when $-G_T M_N^2 = 13.8$ ($-G_T/G_s = 0.949$) in PM1 and at $\rho_B \approx 0.96\rho_0$ when $-G_T M_N^2 = 21.0$ ($-G_T/G_s = 0.819$) in PM2. In the chiral-restored phase $\rho_{SC}^{(\mathrm{II})} \to \infty$ as $-G_T \to 0$, so that the phase transition occurs at any value of $-G_T$. As $-G_T$ increases, the critical density of SP-II, $\rho_{SC}^{(\mathrm{II})}$, becomes smaller, and then it is lower than the CPT density, $\rho_{SC}^{(\mathrm{II})} < \rho_c$, when $-G_T M^2 > 17.7$ ($G_T/G_s < -1.21$) in PM1 and when $-G_T M^2 > 27.6$ ($G_T/G_s < -1.07$) in PM2.

In this work we take the current quark mass to be zero. Realistically the current quark mass is nonzero, and the SC-I and SC-II phase are not distinguished, but qualitative behaviors must be the same. In most cases the SP-I phase must continuously connect with the SP-II phase. However, the SP phase may appear in two different regions as in Fig. 6(a), and three SP states may appear at the same density as in Fig. 4(a): the behaviors must depend on a value of G_T.

IV. SUMMARY

We have studied the spontaneous SP of quark matter in the NJL model with the tensor interaction. There appear two kinds of spin-polarized phases, the SP-I and SP-II phases, where the dynamical quark mass is nonzero and zero, respectively. The SP-I phase appears when the T coupling G_T is negatively large, but the SP-II phase can always appear above the critical density when $G_T < 0$ even though its transition density depends on G_T [12,18].

The SP-I phase can exist in the density region above the *CPT* density and shifts the chiral transition to higher density. On the other hand, the SP-II phase can appear below the *CPT* density. The SP-I and SP-II phases can exist at the same density when $-G_T$ is large. In the present model we cannot discuss the stability of each phase or draw a definite conclusion. However, we can easily suppose that the phase transition between the SP-I and SP-II phases is of the first order.

We have considered an appearance of a nonuniform phase with the AV interaction during the chiral transition, where the pseudoscalar condensate as well as the scalar condensate is nonvanishing, called the dual chiral density wave [13]. The T-type SP must lead to a new type of DCDW, which can appear in the chiral-restored phase. We should study it in the future.

In this paper we treat the moderate density region $\rho_B \lesssim 6\rho_0$, where the NJL model may be useful, and obtain the SP properties in the mean-field framework. In higher density, however, the CSC is brought about by the particle-particle correlation such as the diquark channel, whereas spontaneous magnetization is brought about by the particle-antiparticle or particle-hole correlation. In the CSC phase, the quark mass must be close to the current quark mass, and the T channel interaction may play a more important role than that of the AV channel [14].

In addition, we can apply our approach to the problem of the coexistence of the SP with the CSC. So, one may expect some competition between them, which should be complicated. It is also one of the future problems.

In this paper we have made the discussion only when $G_T < 0$: the spin-polarized phase is isoscalar. When $G_T > 0$, the spin-polarized phase becomes isovector, where the directions of the SP for u- and d-quarks are opposite. The strength of the magnetic field is much larger in the isovector spin-polarized phase than in the isoscalar SP phase because the charge of u- and d-quarks have opposite signs.

Because of Eq. (10), however, the tensor density is maximum at $\rho_u = \rho_d$. When we impose the charge neutrality, the u-quark density becomes smaller than that of d-quark. In the charge neutral system, thus, the SP becomes weaker than that of the present calculation.

In the present work we have discarded the vacuum contribution to the tensor density because its contribution strongly depends on the regularization method. We have demonstrated in Appendix B that the vacuum contribution becomes important at high densities. However, the value of the cutoff parameter is determined to reproduce the dynamical quark mass in the vacuum, but is not related to the spin property, and then the large dependence on the cutoff parameter is not meaningful.

In order to remove the ambiguity we need to use a renormalizable model and to introduce some counterterms to reproduce the vacuum spin susceptibility at zero temperature, which should be determined by other studies such as by the Lattice QCD. It is a future problem.

In this work, furthermore, we have not considered the AV channel of the quark-quark interaction, which can be derived by the Fierz transformation of the one-gluon exchange. The calculation of the spin-polarized phase is very difficult when both the T and AV interactions are introduced because the energy spectrum becomes very complicated. If the weak T interaction is mixed with the AV one, however, the AV-type SP phase appears even when the quark mass is zero; this subject is beyond the scope of this paper.

When the quark mass is small, the tensor density decreases as the AV-type SP becomes larger,[3] and the magnetic field which is produced by the spin current also decreases [12]. However, the magnetic field can be kept to be finite by the tensor mean field even if it is weak. So, the mixing of AV and T interactions may exhibit a new spin polarization in quark matter.

Moreover, the external magnetic field leads to the Landau quantization for quarks. When the strength of the external magnetic field is 10^{18-19} G, the magnetic energy becomes comparable with the Fermi energy, and the Landau quantization affects magnetic properties of the quark matter when the spin-spin interaction is an axial-vector [22] or tensor type [23].

In the future, we hope to extend our formulation for the system including both the AV and T interactions and/or including the external magnetic field.

ACKNOWLEDGMENTS

This work was supported in part by the Grants-in-Aid for the Scientific Research from the Ministry of Education, Science and Culture of Japan (16k05360). T. T. is partially supported by a Grant-in-Aid for Scientific Research on Innovative Areas through No. 24105008 provided by MEXT.

APPENDIX A: DENSITY-DEPENDENT PARTS OF DENSITIES

In this section, we give the detailed expressions of the quark density ρ_q, the scalar density ρ_s, and the tensor density ρ_T with the quark mass M_q, the chemical potential e_F, and the T field $U_T(> 0)$.

[3] $\rho_T \to 0$ when $U_A \to \infty$.

1. Quark densities

When $U_T < e_F - sM_q$ for $s = \pm 1$,

$$\rho_q(s) = \frac{N_d}{2\pi^2}\left\{\frac{1}{6}\sqrt{e_F^2-(M_q+sU_T)^2}\times[2e_F^2-(M_q+sU_T)(2M_q-sU_T)] - \frac{s}{2}U_T e_F^2\left[\frac{\pi}{2}-\sin^{-1}\left(\frac{M_q+sU_T}{e_F}\right)\right]\right\}. \quad \text{(A1)}$$

When $U_T > e_F - sM_q$,

$$\rho_q(+1) = 0, \qquad \rho_q(-1) = \frac{N_d}{4\pi}U_T e_F^2. \quad \text{(A2)}$$

2. Scalar densities

When $U_T < e_F - sM_q$ for $s = \pm 1$,

$$\rho_s(s) = \frac{N_d}{4\pi^2}M_q\left[e_F\sqrt{e_F^2-(M_q+sU_T)^2} - \frac{(M_q+sU_T)^2}{2}\ln\left(\frac{e_F+\sqrt{e_F^2-(M_q+sU_T)^2}}{e_F-\sqrt{e_F^2-(M_q+sU_T)^2}}\right)\right]. \quad \text{(A3)}$$

When $U_T > e_F - sM_q$,

$$\rho_s(\pm 1) = 0. \quad \text{(A4)}$$

3. Tensor density

When $U_T < e_F - M_q$ for $s = 1$ or $U_T < M_q$ for $s = -1$

$$\rho_T(s) = \frac{N_d}{12\pi^2}s\left\{(M_q+sU_T)^2\left(-M_q+\frac{s}{2}U_T\right)\times\ln\left(\frac{e_F+\sqrt{e_F^2-(M_q+sU_T)^2}}{e_F-\sqrt{e_F^2-(M_q+sU_T)^2}}\right) + e_F(M_q-2sU_T)\sqrt{e_F^2-(M_q+sU_T)^2} + e_F^3\sin^{-1}\left(\frac{\sqrt{e_F^2-(U_T+sM_q)^2}}{e_F}\right)\right\}. \quad \text{(A5)}$$

When $U_T > e_F - M_q$ for $s = 1$,

$$\rho_T(+1) = 0. \quad \text{(A6)}$$

When $e_F + M_q > U_T > M_q$ for $s = -1$,

$$\rho_T(-1) = -\frac{N_d}{12\pi^2}\left\{-\frac{1}{2}(U_T-M_q)^2(U_T+2M_q)\times\ln\left(\frac{e_F+\sqrt{e_F^2-(U_T-M_q)^2}}{e_F-\sqrt{e_F^2-(U_T-M_q)^2}}\right) + e_F(2U_T+M_q)\sqrt{e_F^2-(U_T-M_q)^2} + e_F^3\left[\pi-\sin^{-1}\left(\frac{\sqrt{e_F^2-(U_T-M_q)^2}}{e_F}\right)\right]\right\}. \quad \text{(A7)}$$

When $U_T > e_F + M_q$ for $s = -1$,

$$\rho_T(-1) = -\frac{N_d}{12\pi}e_F^3. \quad \text{(A8)}$$

APPENDIX B: VACUUM CONTRIBUTION TO TENSOR FIELD

1. Ambiguities of vacuum contribution

In the paper we mentioned that the vacuum contribution is ambiguous and dependent on the regularization scheme. We explain the reason for this difference with the energy cutoff and the three-dimensional momentum cutoff as examples.

In these regularization schemes, the vacuum part of the tensor density is written as

$$\begin{aligned}\rho_T(V) &= N_d\int\frac{d^4p}{(2\pi)^4}\mathrm{Tr}[i\Sigma_z S_F(p)]\\ &= iN_d\sum_s\int\frac{d^4p}{(2\pi)^4}n_V(\boldsymbol{p},s)\times\frac{4sU_T(-p_0^2-M^2-U_T^2-\boldsymbol{p}_T^2+p_z^2)}{(-2e(\boldsymbol{p},s))[e^2(\boldsymbol{p},1)-e(\boldsymbol{p},-1)^2][p_0+e_s(\boldsymbol{p},s)-i\delta]}\\ &= -N_d\sum_{s=\pm1}\int\frac{d^3p}{(2\pi)^3}n_V(\boldsymbol{p},s)\frac{s\sqrt{\boldsymbol{p}_T^2+M_q^2}+U_T}{e(\boldsymbol{p},s)},\end{aligned} \quad \text{(B1)}$$

where $n_V(\boldsymbol{p},s)$ is an effective momentum distribution for negative energy particles including the cutoff parameter.

In the energy cutoff regularization, we should take $n_V = \Theta[\Lambda_e - e(\boldsymbol{p},s)]$. Apparently the $\rho_T(V)$ is the different

sign of $\rho_T(D)$; in the present choice $\rho_T(D) < 0 < \rho_T(V)$. Namely, the vacuum contribution suppresses the tensor density.

In general the cutoff parameter is taken to be much larger than the Fermi energy, $\Lambda_e \gg E_F$, and the total tensor density becomes positive, $\rho_T(V) + \rho_T(D) > 0$, so that the SP does not appear when $G_T < 0$. When $G_T > 0$, however, the spontaneous SP appears in the vacuum when the cutoff, Λ_e, increases and exceeds a certain critical value; this phenomenon is not thought to have any physical meaning.

In the momentum cutoff regularization, on the other hand, the effective momentum distribution is taken to be $n_V = \Theta(\Lambda_p - |\boldsymbol{p}|)$. When $0 < U_T \ll 1$,

$$\begin{aligned}\rho_T(V) &\approx -N_d \sum_{s=\pm 1} \int \frac{d^3p}{(2\pi)^3} \Theta(\Lambda_p - |\boldsymbol{p}|) \frac{s\sqrt{\boldsymbol{p}_T^2 + M_q^2} + U_T}{E_p} \\ &\quad \times \left(1 - \frac{sU_T\sqrt{\boldsymbol{p}_T^2 + M_q^2}}{E_p^2}\right), \\ &\approx -2N_d U_T \int \frac{d^3p}{(2\pi)^3} \Theta(\Lambda_p - |\boldsymbol{p}|) \frac{p_z^2}{E_p^3} < 0. \end{aligned} \tag{B2}$$

$\rho_T(V)$ has the same sign of $\rho_T(D)$; namely, the vacuum contribution enlarges the tensor density.

The vacuum contribution to the tensor density is determined by the two effects: one is the difference in the volume in the momentum space between the spin-up and the spin-down quarks, and the other is momentum dependence of $\sum_s \bar{u}(\boldsymbol{p}, s)\sigma_{12}u(\boldsymbol{p}, s)$ at the fixed momentum. The two effects have opposite roles: the former reduces the tensor density, and the latter increase it.

In the energy cutoff regularization, the former effect is larger, and the vacuum contribution reduces the SP. In the momentum cutoff regularization, in contrast, the former effect does not exist, and then the vacuum contribution increases the SP.

When $\Lambda_{e,p} \gg M_q$ and $U_T \ll 1$, the vacuum contribution becomes $\rho_T(V) \approx N_d U_T \Lambda_e^2/2\pi^2$ for the energy cutoff and $\rho_T(V) \approx -N_d U_T \Lambda_p^2/3\pi^2$ for the momentum cutoff. Both results are proportional to the square of the cutoff parameter although the signs of the two results are opposite.

2. Spin polarization with vacuum contribution

In this section, we discuss the vacuum polarization in the proper time regularization.

The vacuum contribution is given by

$$\begin{aligned}\rho_T(V) &= \frac{N_d}{4\pi^2}\Lambda^2 \int_{M-U_T}^{M+U_T} dE_T F_1\left(\frac{E_T^2}{\Lambda^2}\right) \\ &\quad + \frac{N_d}{8\pi^2} U_T \Lambda^2 \sum_s F_2\left[\frac{(M + sU_T)^2}{\Lambda^2}\right]. \end{aligned} \tag{B3}$$

In the limit of $\Lambda \to \infty$, the tensor density becomes

$$\begin{aligned}\rho_T(V) &\approx \frac{N_d}{4\pi^2}\left\{\Lambda^2 U_T + \left(M_q^2 U_T - \frac{1}{3}U_T^3\right)\ln\frac{\Lambda^2}{|M_q^2 - U_T^2|}\right. \\ &\quad \left. - \frac{1}{3}M_q^3 \ln\left(\frac{M_q + U_T}{M_q - U_T}\right)^2 + \frac{1}{3}M_q^2 U_T - \frac{5}{9}U_T^3\right\}. \end{aligned} \tag{B4}$$

When $U_T \ll M_q$, in addition,

$$\begin{aligned}\rho_T(V) &\approx \frac{N_d}{4\pi^2}\left\{\Lambda^2 U_T + \left(M_q^2 U_T - \frac{1}{3}U_T^3\right)\ln\frac{\Lambda^2}{M_q^2}\right. \\ &\quad \left. - M_q^2 U_T - \frac{4}{9}U_T^3\right\}. \end{aligned} \tag{B5}$$

Thus, the terms proportional to U_T, U_T^3, and $M_q^2 U_T$ diverge in the limit of $\Lambda \to \infty$.

The above equation shows us that the spin susceptibility proportional to $\partial\rho_T/\partial U_T$ has a very large value at any density, and the SP does not appear in the chiral-broken phase.

When $M_q = 0$ and $U_T \ll 1$, it becomes $\rho_T(V) \approx N_d U_T \Lambda^2/4\pi^2$ and $\rho_T(D) \approx -N_d U_T p_F^2/2\pi^2$, and the condition of the SP becomes

$$p_F^2 \geq \frac{\Lambda^2}{2} - \frac{2\pi^2}{G_T}, \tag{B6}$$

which is strongly dependent on the cutoff parameter Λ.

In the field theory, the divergent terms are renormalized to be physical values. In the NJL model, the cutoff parameter is taken to be finite, and determined by the quark mass at zero density. On the other hand we cannot relate the vacuum part of the tensor density with any physical quantity. In addition, even the sign of this part depends on the regularization method. We cannot believe such a large contribution from the vacuum.

In the present model the term proportional to Λ^2 makes $\rho_T(V)$ extraordinarily large. In the AV-type SP phase [13], on the other hand, the vacuum contribution of the AV density under the AV field, U_A, is written, when $|U_A| \ll M_q \ll \Lambda$, as

$$\rho_A(V) \approx \frac{N_d}{\pi^2} U_A M_q^2 \ln\left(\frac{\Lambda}{M_q}\right). \tag{B7}$$

We see that this vacuum contribution in the AV-type SP [13] does not affect the final result as largely as that of the T-type SP.

As shown in the energy cutoff calculations in Appendix B 1, the term proportional to Λ^2 indicates a contribution from the surface area of the integration in the

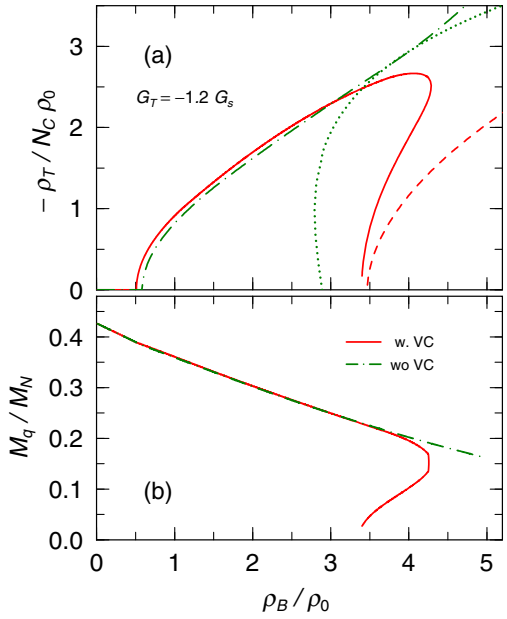

FIG. 8. The tensor density normalized by (a) the normal nuclear matter density and (b) the dynamical quark mass with PM1 and $G_T = -G_s$. The dotted-dashed and solid lines represent the results with and without the vacuum contribution (VC), respectively. In panel (a), the dotted and dashed lines indicate the tensor density with and without VC in the chiral-restored phases, respectively.

region restricted with the cutoff parameter in the momentum space, and it must be removed by the renormalization.

So, we examine the vacuum contribution by removing the term proportional to Λ^2. For this purpose we introduce an additional counterterm, β_T, and define the renormalized thermodynamical potential density as

$$\Omega_R = \Omega_{\rm vac} - \frac{1}{2}\beta_T U_T^2, \tag{B8}$$

which gives the renormalization vacuum tensor density as $\rho_T(R) = \rho_T(V) - \beta_T U_T$. Note that we can define the additional term in the above equation in a Lorentz covariant way by rewriting U_T^2 in the tensor field including six independent components, although this modification does not change the result.

In order to examine the vacuum effects, here, we choose β_T to set the vacuum contribution to be zero at $\rho_B = 0$ and compare those results with those without the vacuum effect.

The Lattice QCD calculation has shown that the negative magnetic susceptibility at the zero temperature limit is zero [24] or negative [25]. The magnetic susceptibility is proportional to the spin susceptibility, and hence our choice is reasonable for a test calculation.

Then, we take β_T to be

$$\beta_T = \frac{N_d}{4\pi^2}\Lambda^2\left[2F_1\left(\frac{M_0^2}{\Lambda^2}\right) + F_2\left(\frac{M_0^2}{\Lambda^2}\right)\right], \tag{B9}$$

where M_0 is the dynamical quark mass at $\rho_B = 0$.

In Fig. 8 we show the tensor density normalized by (a) the normal nuclear matter density $\rho_T/(N_c\rho_0)$ and (b) the dynamical quark mass M_q with PM1 and $G_T = -1.2G_s$. The solid and dotted-dashed lines represent the results without and with the vacuum contribution, respectively.

In the density region, $\rho_B \lesssim \rho_c$, the results with the vacuum contribution are almost the same as those without the vacuum contribution. In the density region, $\rho_B \gtrsim \rho_c$, however, the SP ratio is larger than that without the vacuum contribution, and the SP-I phase survives when the vacuum contribution is included. The vacuum polarization has a role to keep the quark mass finite in the SP phase in the high-density region.

These large vacuum contributions are considered to come from the second term of Eq. (B5), which is proportional to $\ln(\Lambda^2/M_q^2)$, and becomes larger as the dynamical quark mass decreases. This contribution cannot be removed by a usual renormalization process because a related counterterm must be proportional to $M_q^2 U_T^2$, which becomes smaller with the decrease of M_q.

[1] For a review, see G. Chanmugam, Annu. Rev. Astron. Astrophys. **30**, 143 (1992).
[2] P. M. Woods and C. Thompson, *Compact stellar X-ray sources*, edited by W. Lewin and M. van der Klis (Cambridge Univ. Press, Cambridge U.K, 2006), p. 547; A. K. Harding and D. Lai, Rep. Prog. Phys. **69**, 2631 (2006).
[3] P. Braun-Munzinger and J. Stachel, Nature (London) **448**, 302 (2007).
[4] For recent reviews, see F. Weber, Prog. Part. Nucl. Phys. **54**, 193 (2005); D. Page and S. Reddy, Annu. Rev. Nucl. Part. Sci. **56**, 327 (2006); J. M. Lattimer and M. Prakash, Phys. Rep. **442**, 109 (2007).
[5] T. Schaefer, arXiv:hep-ph/0509068; P. Braun-Munzinger and J. Wambach, Rev. Mod. Phys. **81**, 1031 (2009).
[6] For a recent review, see M. G. Alford, A. Schmitt, K. Rajagopal, and T. Schaefer, Rev. Mod. Phys. **80**, 1455 (2008).
[7] T. Tatsumi, Phys. Lett. B **489**, 280 (2000); T. Tatsumi, E. Nakano, and K. Nawa, *Dark Matter* (Nova Science Pub., New York, 2006), p. 39.
[8] F. Bloch, Z. Phys. **57**, 545 (1929).
[9] C. Herring, *Exchange Interactions among Itinerant Electrons: Magnetism IV* (Academic Press, New York, 1966); K. Yoshida, *Theory of Magnetism* (Springer, Berlin, 1998).

[10] T. Moriya, *Spin Fluctuations in Itinerant Electron Magnetism* (Springer, New York, 1985).
[11] T. Maruyama and T. Tatsumi, Nucl. Phys. **A693**, 710 (2001).
[12] T. Maruyama, E. Nakano, and T. Tatsumi, *Horizons in World Physics* (Nova Science, NY, 2011), Vol. 276, Chap. 7.
[13] E. Nakano and T. Tatsumi, Phys. Rev. D **71**, 114006 (2005).
[14] E. Nakano, T. Maruyama, and T. Tatsumi, Phys. Rev. D **68**, 105001 (2003).
[15] R. Yoshiike and T. Tatsumi, Phys. Rev. D **92**, 116009 (2015).
[16] Y. Nambu and G. Jona-Lasinio, Phys. Rev. **122**, 345 (1961).
[17] S. Maedan, Prog. Theor. Phys. **118**, 729 (2007).
[18] Y. Tsue, J. de. Providencia, C. Providencia, and M. Yamamura, Prog. Theor. Phys. **128**, 507 (2012).
[19] K. Tsushima, T. Maruyama, and A. Faessler, Nucl. Phys. **A535**, 497 (1991).
[20] T. Maruyama, K. Tsushima, and A. Faessler, Nucl. Phys. **A537**, 303 (1992).
[21] J. Schwinger, Phys. Rev. **82**, 664 (1951).
[22] R. Yoshiike, K. Nishiyama, and T. Tatsumi, Acta Phys. Pol. B Proc. Suppl. **9**, 523 (2016).
[23] Y. Tsue, J. da Providência, C. Providência, M. Yamamura, and H. Bohr, Int. J. Mod. Phys. E **E25**, 1650106 (2016).
[24] C. Bonati, M. D'Elia, M. Mariti, F. Negro, and F. Sanfilippo, Phys. Rev. D **89**, 054506 (2014).
[25] G. S. Bali, F. Bruckmann, M. Constantinou, M. Costa, G. Endrodi, S. D. Katz, H. Panagopoulos, and A. Schaefer, Phys. Rev. D **86**, 094512 (2012).